VOL. 19, NO. 2, JANUARY 2024 ISSN 1819-6608
ARPN Journal of Engineering and Applied Sciences

www.arpnjournals.com

# A STUDY OF SWIRL FLOW MEASUREMENTS IN A CYLINDER UNDER AN INTAKE FLOW SIMILAR TO AN ENGINE OPERATING CONDITION USING A ROTATING SLIT DISK VALVE

Dase San Oh[1] and Choong Hoon Lee[2]
[1]Defense Agency for Technology and Quality, Daejeon, Korea
[2]Department of Mechanical and Automotive Engineering, Seoul National University of Science and Technology, Seoul, Korea
E-Mail: chlee5@seoultech.ac.kr

**ABSTRACT**

A new swirl measurement system was developed by installing bevel gears and a slit rotary valve into an impulse-type swirl measurement system of the type traditionally used to measure the swirl ratio and flow coefficient of engine intake ports. When operating this new swirl measurement system, it was confirmed that the characteristics of the intake air flow rate to the cylinders were similar to those of a typical operating engine condition. When the valve lift was limited to the cam angle range of 160 to 200 (the valve lift is maximized at a cam angle of 180°), the flow coefficient $C_f$ increased as the cam angle increased under a constant camshaft rotation speed. Moreover, as the rotation speed of the camshaft increased, the $C_f$ value decreased slightly. The swirl ratio $N_R$ in the cam angle range of 160 to 200 showed a nearly constant value with an increase of the cam angle at a constant camshaft rotation speed. There were also no significant changes in $C_f$ with an increase in the camshaft rotation speed. $N_R$ measurement results while changing the camshaft rotation speed cannot be obtained by the traditional impulse swirl measurement method. $N_R$ measurement results with the new swirl measurement system can be used as basic data when calculating spray dispersion characteristics considering the engine rotation speed.

**Keywords:** swirl ratio, flow coefficient, intake port, engine operating condition, unsteady flow condition, rotating slit disk valve.

Manuscript Received 12 December 2023; Revised 25 February 2024; Published 18 March 2024

## INTRODUCTION

An important parameter when seeking to improve diesel engine performance is the rapid mixing of fuel and air in the combustion chamber. In a diesel engine, the most important factors with the greatest influence on the fuel-air mix are the fuel injection pressure and the swirl flow in the combustion chamber as generated by the intake port.

In general, increasing the injection pressure of a diesel injector promotes fuel-air mixing because by increasing the fuel injection pressure, the atomization of the fuel spray is promoted by the high injection pressure. In addition, when the fuel injection pressure is high, the diameter of the injector nozzle is smaller, which further promotes the atomization of the fuel spray [1-3].

Another important parameter influencing the mixing of the fuel and air in a diesel engine is the swirl flow in the engine combustion chamber. The swirl flow is created by the intake port. In a diesel engine, fuel is injected toward the combustion chamber wall when the piston has almost reached the top dead center. At this point, the swirl flow in the piston combustion chamber deflects the fuel spray injected from the injector in a tangential direction in the combustion chamber, thus promoting the mixing of fuel and air. In a related study, Lee [4] studied the diesel spray dispersion characteristics with swirl flow using a visualization method. Hiroyasu et al. [5, 6] and Klein-Douwell [7] utilized an experimental method to assess the dispersion characteristics of diesel sprays. Zhang et al. [8], Gao et al. [9], and Du et al. [10] studied the mixing characteristics of diesel sprays using the LAS (laser absorption scattering) technique. Felton *et al.* [11] studied the mixing characteristics of diesel sprays using the LIFF (laser induced exciplex fluorescence) method and Rabenstein *et al.* [12] used the Raman scattering method to investigate diesel spray mixing. Nawi *et al.* [13] studied the mixing characteristics of diesel sprays by analyzing the behavior of droplets using a shadowgraph method.

Engine manufacturers regularly measure the intake port swirl ratio to maintain target engine performance levels. In other words, when a cylinder head is produced, a certain quantity is periodically sampled to measure the swirl ratio of the intake port. In this way, it is possible to reduce performance variations in the engines being produced. Currently, two methods of measuring the swirl ratio are commonly used by engine manufacturers. The first [14] measures the number of revolutions by installing a paddle in the engine cylinder in what is known as the AVL method. The second is the impulse method [15], also called the Ricardo method.

The intake air flow in the engine cylinder is unsteady. Both the paddle method and the impulse method measure the intake port swirl ratio under a steady flow condition. The swirl ratio measured by these two methods has a problem in that it does not reflect the actual unsteady swirl flow in the engine cylinder. The paddle method and impulse methods are used by engine makers because it is very difficult to measure the intake port swirl ratio under actual engine operation conditions.

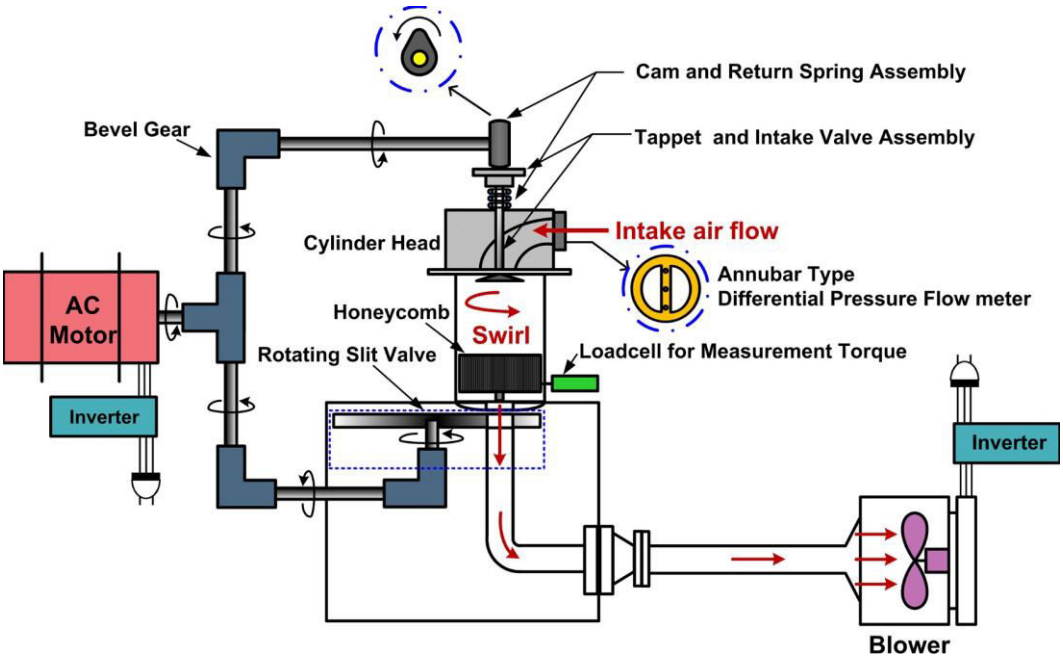


**Figure-1.** Experimental setup for measuring the swirl ratio of an intake port under an intake air flow condition similarto that of an engine operating condition.

To reflect actual engine intake flow conditions, Kim and Lee [16] attempted to measure the swirl ratio by modifying the paddle-type swirl measuring device. They used a step motor instead of a micrometer to adjust the valve lift. With the step motor, valve lift adjustments, and swirl ratio measurements are automated and the measurement time is dramatically reduced. However, the conditions in their method are very different from the actual engine operating conditions because the intake flow is close to a steady flow when measuring the swirl ratio. Oh, and Lee [17] sought to measure the swirl ratio by modifying the impulse-type swirl ratio measurement system. They directly rotated the camshaft to adjust the valve lift. By rotating the camshaft, valve lift adjustments, and swirl ratio measurements were automated, and the measurement time was also dramatically shortened. However, when measuring the swirl ratio using their method, the generated intake flow in the cylinder is different from the actual engine intake flow in which a four-stroke process (suction- compression-expansion-exhaust) is utilized. Hence, their method has a problem in that the suction flow to the cylinder is continuously maintained throughout all four strokes.

Currently, few systems measure the swirl ratio under an unsteady flow condition close to the actual engine intake flow. To overcome the problems of existing technology used to measure the swirl ratio and flow coefficient, a new swirl measurement system is developed here where the intake flow into the cylinder occurs intermittently at every engine cycle. To make the air intake process in the newly developed swirl ratio measurement system equivalent to the actual engine intake process, several bevel gears and a rotating slit disk valve were devised and used in this study. The swirl ratio measurement system developed in this study greatly reduces the measurement time and enables repeated measurements, in turn enabling the statistical processing of the measurement data.

## EXPERIMENTS

Figure-1 shows a schematic diagram of the experimental setup used in this study. Oh, and Lee [17] rotated the camshaft with an AC motor. In this study, the experimental system of Oh and Lee [17] was modified by additionally installing three L-type bevel gears, one T-type bevel gear, and a slit rotation valve to control the opening and closing of the intake air flow to the cylinder. The bevel gears serve to synchronize both the camshaft rotational position and the slit rotational valve rotational position. As the camshaft rotates, the intake valve lifts along the cam profile and at the same time, the slit rotation valve rotates synchronously, causing air intake in the cylinder to occur intermittently at every engine cycle. An average pitot flowmeter (APT flowmeter) was installed at the intake port inlet of the cylinder head, and a differential pressure sensor was installed to measure the differential pressure at the APT flowmeter.

Figure-2 shows a 3D detailed conceptual diagram of the valve lift control scheme (Figure-2(a)), including the encoder for measuring the camshaft rotation position, the swirl measurement system in the cylinder (Figure-2(b)),and the slit rotation valve (Figure-2(c)). As shown in Figure-1, the AC motor rotation is branched into two directions through the T-type bevel gear. The AC-motor rotation is transferred to both the camshaft through an L-type bevel gear and the slit rotating valve at the bottom of the cylinder through another L-type bevel gear.

Accordingly, the rotation position of the slit rotation valve and the rotation position of the camshaft completely coincide. The opening area between the intake

valve and the valve seat with the camshaft rotation and the opening slit area with the rotation of the slit rotation valve are substantially proportional to each other.

As shown in Figure-2(b), the impulse torque measurement system consists of a honeycomb matrix, a blade, and a load cell. When air enters the cylinder through the intake valve, the tangential flow created by the helical port impinges on the honeycomb matrix. Due to this, the force in the tangential direction is transmitted to the load cell through the rod and knife edge. The gap between the cylinder and the outer peripheral surface of the honeycomb structure is within 1 mm. That is almost no air leaks through the axial gap between the cylinder and the honeycomb structure, which makes the load cell sense most of the tangential momentum in the cylinder. The honeycomb structure is mounted on a circular bracket, and the central axis of the circular bracket is combined with a radial bearing. Accordingly, the force due to the tangential flow acting on the honeycomb structure is converted into a circular bracket rotational force. A rod was attached to the outer circumferential surface of the circular bracket in the radial outward direction. The rod passes through a hole machined in the cylinder and is combined with the knife edge. The knife edge stays in contact with the load cell. When there is no flow in the cylinder through the intake valve, the honeycomb matrix is in a no-load condition. By multiplying the tangential force measured by the load cell by the distance from the center of the cylinder to the point of contact between the blade and the load cell, the tangential torque caused by the air flow in the cylinder can be calculated. The load cell was calibrated using a scale and a weight and was then installed in the experimental system.

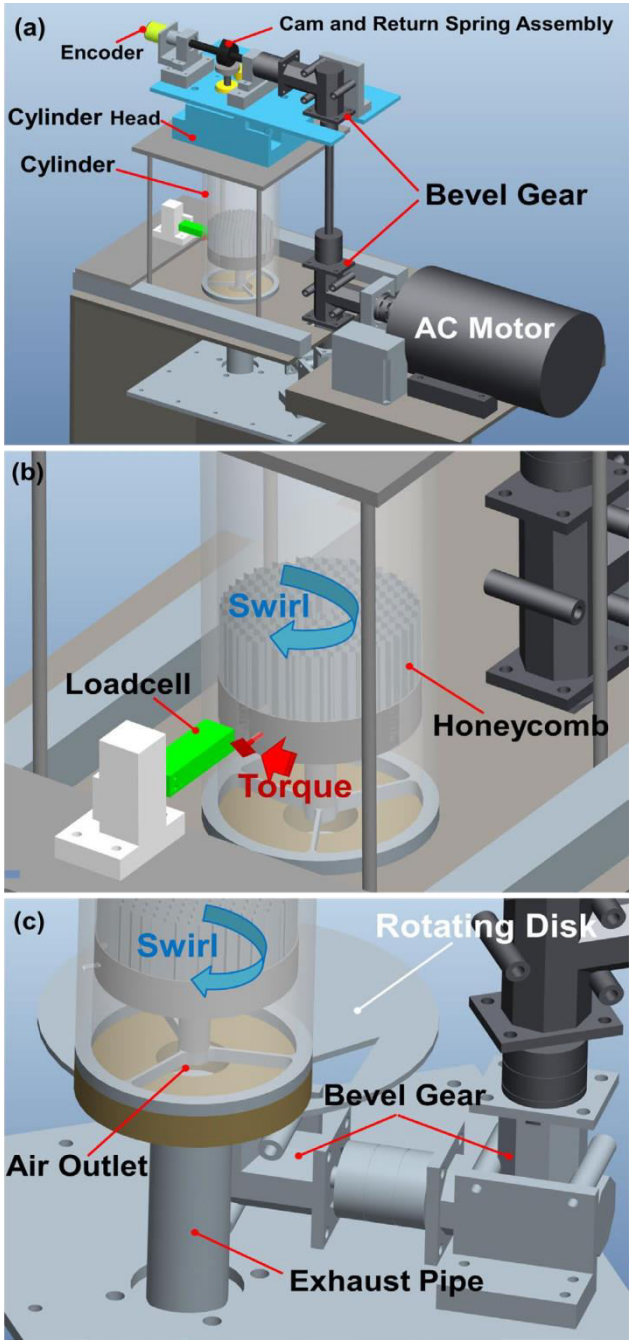


**Figure-2.** 3D view of the experimental system: (a) experiment schematics, (b) measurement of the tangential torque induced by the swirl flow using a loadcell in detail, and (c) rotating slit disk in detail.

As shown in Figure-3, a slit rotation valve was installed at the bottom of the cylinder to suck air into the cylinder intermittently with the camshaft rotation position. It was designed so that air can be sucked into the cylinder only while the slit of the crescent-shaped slit rotary valve and the fixed round pipe overlap. The camshaft and the slit rotation valve rotate in a synchronized manner, and when the intake valve starts to open by the camshaft, the overlapping of the slit rotation valve and the round pipe begins, as shown in Figure-3(a). From this point, air

begins to be sucked into the cylinder. The air intake process takes place over a 90° cam angle. This means that the overlap of the slit rotary valve and the round pipe occurs over a 90° cam angle. In Figure-3(b), the position where the overlap area between the slit rotary valve and the round pipe is maximized is at a cam angle of 45°. After the valve overlap is maximized, the overlap area starts to decrease. When the cam angle is rotated by 90° (see Figure-3(c)), valve overlapping ends, and air intake into the cylinder is stopped. This intake air process can be flexibly changed by adjusting the overlap section of the slit rotary valve and the round pipe. The air intake flow into the cylinder occurs intermittently for each camshaft revolution.

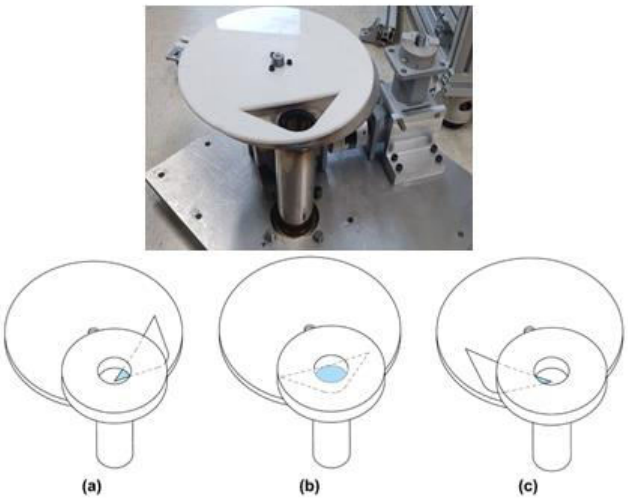


**Figure-3.** Effective air flow area according to the angular position of the rotating slit disk: (a) start of the opening process (b) opened to the maximum amount and (c) closure of the opening.

Figure-4 shows a conceptual diagram of the measurement of two differential pressure sensor signals, the load cell signals, and the encoder signals. The figure shows the APT flowmeter installed to measure the intake air mass flow rate into the cylinder and the corresponding cross-sectional shape. To measure the static pressure inside the cylinder, one pressure tap of the differential pressure sensor (#2) was connected through a hole in the cylinder wall, and the other pressure tap was exposed to atmospheric pressure. To detect the differential pressure between the upstream pressure and the downstream pressure of the APT flowmeter, the upstream pressure of the APT flowmeter is applied to one tap of the differential pressure sensor (#1), and the downstream pressure of the APT flowmeter is applied to the other tap of the differential pressure sensor (#1). All sensor signals were recorded using a four-channel digital oscilloscope.

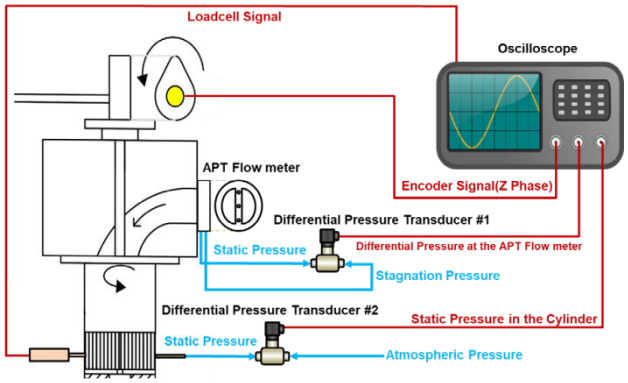


**Figure-4.** Diagram for measuring the cam position by the encoder and intake air mass flow rate by pressure sensors.

The swirl measurement process is summarized as follows. First, the blower motor rotation speed is set by an inverter for suctioning a constant mass flow rate corresponding to that at a constant engine speed. At the same time, the blower rotation speed was controlled to increase the intake air mass flow rate in proportion to the rotation speed of the AC motor to drive the camshaft. When the AC motor rotates, the camshaft and the slit rotation valve are synchronically rotated by a combination of one T-type bevel gear and three L-type bevel gears. While the camshaft rotates at a constant speed, two differential pressure sensor signals, an encoder signal, and a torque sensor signal are recorded with the four-channel oscilloscope. All sensor signals were simultaneously measured with an interval of about 1° or less at the camshaft angle. The camshaft rotational speed was controlled at 150, 200, 250, and 300 rpm and was continuously measured over 20 rotations at each rotational speed.

## RESULTS AND DISCUSSIONS

Figure-5 shows the average of the differential pressure ($P_{static}$) between atmospheric pressure and in-cylinder pressure measured 20 times at an interval of about 1° or less at the cam angle. When the experimental system is operated, the pressure in the cylinder is lower than the atmospheric pressure; that is, negative pressure relative to the atmospheric pressure forms. The negative sign added to this negative pressure is $P_{static}$. A large $P_{static}$ value means that the magnitude of the negative pressure in the cylinder is large. As the rotation speed of the camshaft increased, $P_{static}$ increased over the entire cam angle range.

The reason for such a result is that for the same valve lift (same cam angle), as the camshaft rotation speed increases,the intake air mass flow rate increases, and thus the pressure loss through the intake valve increases. The maximum $P_{static}$ values at the camshaft rotation speeds of 150 rpm, 200 rpm, 250 rpm, and 300 rpm were 0.4 kPa, 0.7 kPa, 1.3 kPa, and 2.2 kPa, respectively. The maximum Pstatic value generally appeared at the cam angle of 180°, and the valve lift at the position of the cam angle of 180° was maximized. In the cam angle ranges of 0-120° and

240-360°, the intake valve is closed and air intake into the cylinder is stopped; thus, $P_{static}$ was very close to 0.

Figure-6 shows the measurement results of the differential pressure ($\Delta P_{up\text{-}down}$) between the upstream pressure and the downstream pressure in the APT flowmeter. The $\Delta P_{up\text{-}down}$ values with the cam angle when maintaining camshaft rotational speeds of 150 rpm, 200 rpm, 250 rpm, and 300 rpm constantly are shown. The $\Delta P_{up\text{-}down}$ measurement results are similar to those of the Pstatic measurement result shown in Figure-5. The $\Delta P_{up\text{-}down}$ value is generally smaller than the $P_{static}$ value. The maximum $\Delta P_{up\text{-}down}$ values at the camshaft rotation speeds of 150 rpm, 200 rpm, 250 rpm, and 300 rpm were 0.3 kPa, 0.6 kPa, 0.9 kPa, and 1.5 kPa, respectively. The cam angle showing the maximum $\Delta P_{up\text{-}down}$ value for each camshaft

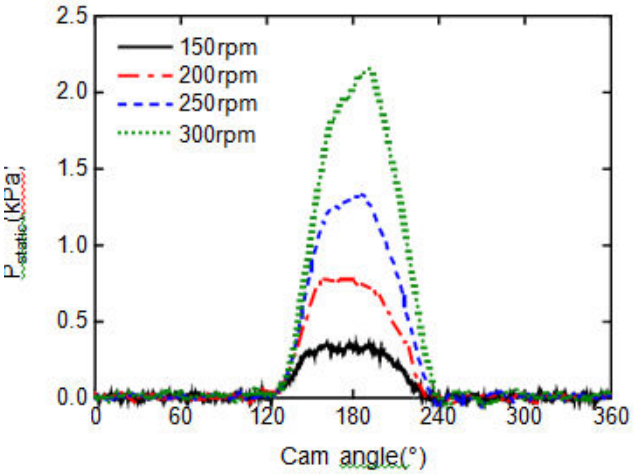


**Figure-5.** Measured static pressure in a cylinder with the camshaft angle at various camshaft rotation speeds.

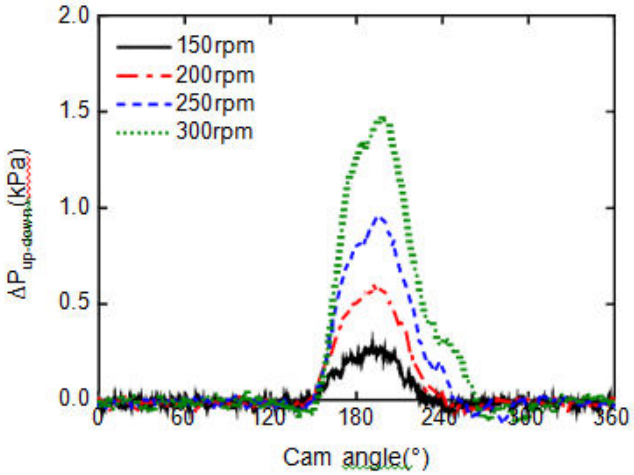


**Figure-6.** Measured differential pressure between upstream and downstream at the APT flow meter with the camshaft angle at various camshaft rotation speeds.

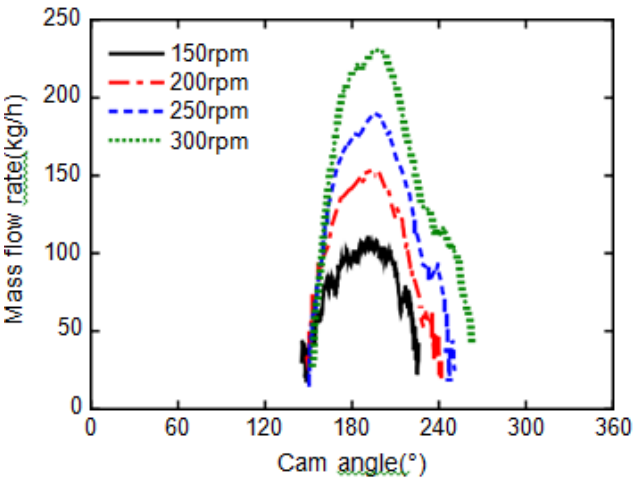


**Figure-7.** Calculated mass flow rate at the APT flow meter with the camshaft angle at various camshaft rotation speeds.

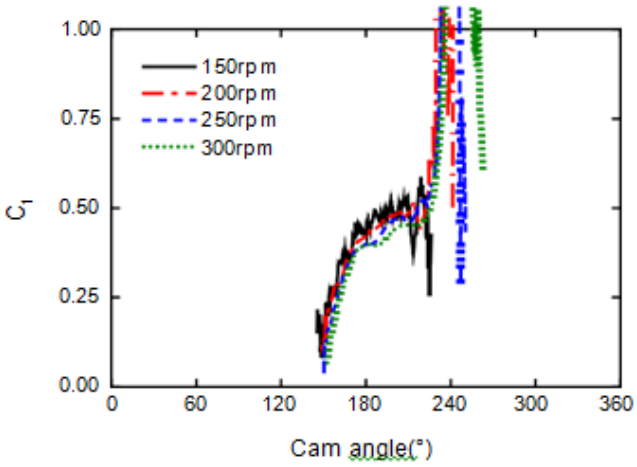


(a)

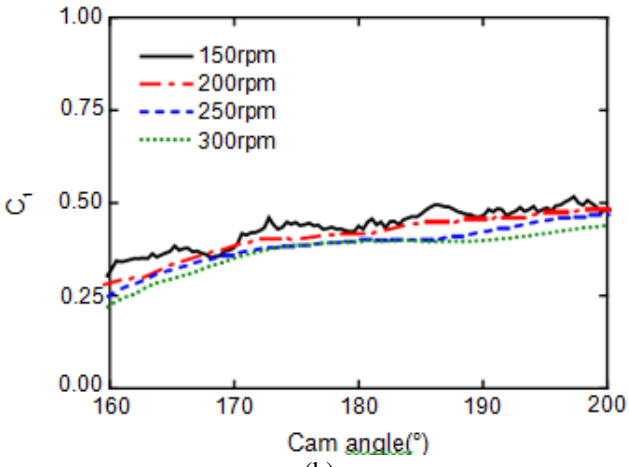


(b)

**Figure-8.** Flow coefficient with the camshaft angle at various camshaft rotation speeds: (a) cam angle Range of 0° to 360° and (b) cam angle range of 160° to 200°.

rotation speed was found to be close to 190°, which is slightly larger than 180° where the maximum $P_{static}$ appears. This result stems from the different measurement positions of $\Delta P_{up\text{-}down}$ and $P_{static}$. Both $P_{static}$ and $\Delta P_{up\text{-}down}$ increased until the cam angle approached 180° and decreased past a cam angle of approximately 180°. In the cam angle ranges of both 0~120° and 240~360°, the intake valve is completely closed and air intake through the slit rotation valve is blocked; therefore, air intake into the cylinder is stopped. Because the intake air flow rate into the cylinder was increased in proportion to the camshaft rotation speed, the maximum $P_{static}$ and $\Delta P_{up\text{-}down}$ values increased with the camshaft rotation speed.

Figure-7 shows the results of the intake air mass flow rate measured with the APT flowmeter. The measurement results of the intake air mass flow rate with the cam angle are shown when the camshaft rotation speed is kept constant at 150 rpm, 200 rpm, 250 rpm, and 300 rpm. The measured intake air mass flow rate results shown in Figure-7 show trends similar to those of $\Delta P_{up\text{-}down}$ shown in Figure-6. The maximum value of the intake air mass flow rate for each rotation speed appeared in the 190~200° cam angle range, identical to the cam angle range where the maximum value of differential pressure measured at the APT flowmeter appeared. At the camshaft speeds of 150 rpm, 200 rpm, 250 rpm, and 300 rpm, the maximum intake air volumes were found to be 111.3 kg/h, 153.4 kg/h, 190.1 kg/h, and 231.7 kg/h, respectively.

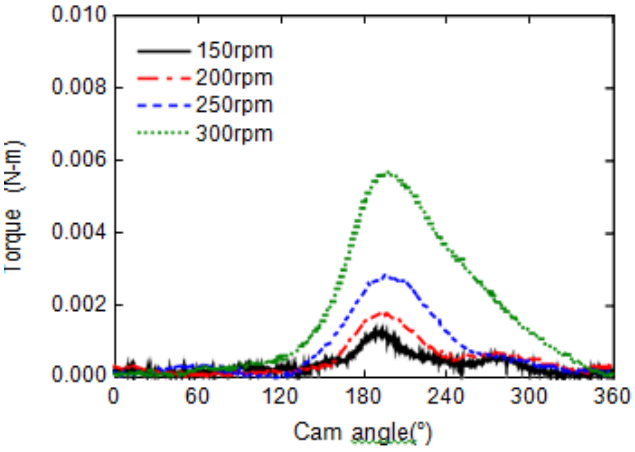


**Figure-9.** Measured torque with the camshaft angle at various camshaft rotation speeds.

increases gradually from 0.25 to 0.39-0.49 as the cam angle increases from 160°, where the intake valve starts to open, to 200°. $C_f$ increases with an increase in the cam angle due to the increase of the valve lift with the increased cam angle. As the rotational speed of the camshaft increases, $C_f$ decreases slightly. The decrease of $C_f$ with the increase of the rotational speed of the camshaft is due to the increased pressure loss with the increase in the intake air mass flow rate.

Figure-9 shows the average of the impulse torque with the cam angle when the camshaft rotation speed is about 1° or less of the cam angle while the camshaft rotated 20 times. At each camshaft rotational speed, the flow coefficient $C_f$ of the cylinder head intake port is calculated using Eq. (1) [18]. In Eq. (1), the subscripts o and d indicate the inlet and outlet of the intake valve, respectively. k and R are the specific heat ratios of the air and gas constants, respectively, and $\dot{m}$, $P_o$, $P_d$, and $T_o$ are likewise the intake air mass flow rate, atmospheric pressure, surge tank pressure, and intake air temperature. A is the flow path area created by the gap between the intake valve and the valve seat. The size of A changes as the valve lift changes. Here, for convenience of the calculation, the area of the circle calculated by the intake valve diameter assumes a constant value. The flow coefficient $C_f$ can be calculated by measuring $\dot{m}$, $P_o$, $P_d$, and $T_o$ under each experimental condition.

Figure-8(a) shows the $C_f$ results calculated from impulse torque changed for each change in the cam angle. The impulse torque peaked when the clearance between the intake valve and the valve seat was the largest (when the valve lift reached its maximum) because the intake air flow velocity was the highest. Also, as the camshaft rotation speed increased, the impulse torque increased due to the increase in the intake air mass flow rate. At each camshaft rotation speed, the impulse torque peak does not appear at the cam angle position of 180° but appears near 185-195° because the impulse torque measurement is taken at a certain distance downward from the intake valve. The maximum impulse torque values at the camshaft rotational speeds of 150, 200, 250, and 300 rpm were 0.0013, 0.0019, 0.0029, and 0.0057 N·m, respectively.

Eq. (1). The variation of $C_f$ with the cam angle is shown as the camshaft rotation speed was kept constant at 150, 200, 250, and 300 rpm. In both the cam angle range of 0 to 150° and the cam angle range of 240 to 360°, the clearance between the intake valve and the valve seat is reduced, which significantly reduces the intake air mass flow rate. The intake mass flow rate in these cam angle ranges became unstable; thus, the fluctuation of $C_f$ became too broad. Figure-8(b) shows a magnified result of $C_f$ in the cam angle range of 160-200°. Under the condition in which the camshaft rotation speed is kept constant, $C_f$

The swirl ratio $N_R$, which is a dimensionless number, can be calculated from Eq. (2) [18]. In Eq. (2), G, $\dot{m}$, and B are the measured impulse torque, the intake air mass flow rate, and the cylinder bore, respectively. The ideal intake air flow velocity through the intake valve Vis is calculated from Eq. (3).

$$C_f A P_o \sqrt{\frac{2}{RT_o}} \sqrt{\frac{k}{k-1}} \left(\frac{P_d}{P_o}\right)^{\frac{2}{k}} \left(\frac{P_d}{P_o}\right)^{\frac{k+1}{k}} \quad (1)$$

$$N_R \equiv \frac{8G}{\dot{m}\, BV_{is}} \quad (2)$$

$$V_{is} = \sqrt{\frac{2k}{k-1} \times \frac{P_o}{\rho_o}\left[1 - \left(\frac{P_d}{P_o}\right)^{\frac{k-1}{k}}\right]} \quad (3)$$

result with the camshaft rotation speed shown in Figure-10(b) cannot be obtained with existing traditional swirl measurement methods, such as the paddle method or the impulse method. The NR values with the engine speed change can be used as basic data when calculating Figure-10(a) shows the NR value with the cam angle when the camshaft rotation speed is kept constant. In the cam angle ranges of 0~150° and 240~360°, the clearance of the intake valve and the valve seat is reduced; therefore, the intake air mass flow rate is greatly reduced, which results in an unstable intake air flow rate through the intake valve. For this reason, the fluctuation of the impulse torque became too broad in these cam angle ranges; the NR value is displayed in Figure-10(a). Figure- 10(b) shows a magnified result of NR in the cam angle range of 160-200°. As the cam angle increases from 160° to 200°, NR spans from 0.05 to 0.12. The resulting NR shown in Figure-10(b) means that under the condition of a constant camshaft rotation speed, the NR value shows a nearly constant value with changes in the cam angle. Although there is a limitation here in that the experiment was not conducted at a sufficiently high camshaft rotational speed, there is no significant change in the NR value with an increase in the camshaft rotational speed. In particular, the NR values at 250 and 300 rpm show nearly identical with the cam angle change. The NR measurement

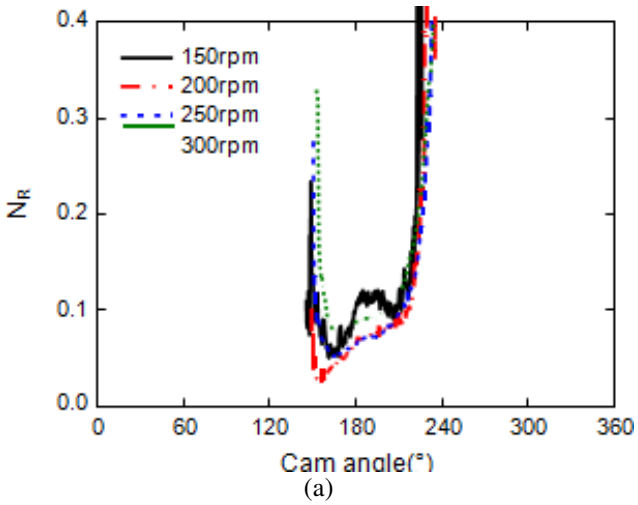

(a)

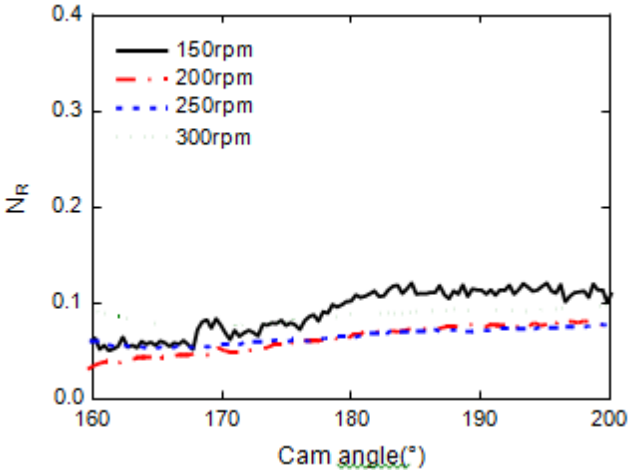

(b)

**Figure-10.** Swirl ratio NR with the camshaft angle at various camshaft rotation speeds: (a) cam angle rangeof 0° to 360° and (b) cam angle range of 160° to 200°. spray dispersion characteristics with the engine rotationspeed.

## CONCLUSIONS

Four bevel gears and a slit rotary valve were installed in a conventional impulse-type swirl measurement system that measures the intake port swirl ratio and flow coefficient under steady flow conditions such that the intake air flow into the cylinder closely approximates the actual operating conditions of an engine. As a result of experimenting to measure the swirl ratio and flow coefficient of the intake port using the newly constructed device, the following conclusions were obtained.

It was confirmed that when the camshaft was rotated by installing four bevel gears and a slit rotation valve in the traditional impulse swirl measurement system, the intake flow characteristics into the cylinder were nearly identical to those of an operating engine.

When the valve lift is limited to the cam angle range of 160-200, which is the range at a cam angle position of approximately 180° at the maximum valve lift, the flow coefficient Cf increases as the cam angle increases at a constant camshaft rotation speed. Also, as the rotation speed of the camshaft increases, the Cf value decreases slightly.

When the valve lift is limited to the cam angle range of 160-200, which is the range at a cam angle position of approximately 180° at the maximum valve lift, the swirl ratio NR showed a nearly constant value with changes in the cam angle. There was no significant change in the NR value with an increase in the camshaft rotation speed.

## REFERENCES

[1] T. Shimada, T. Shoji and Y. Takeda. 1989. The Effect of Fuel Injection Pressure on Diesel Engine Performance, SAE Paper 891919.

[2] S. Kobayashi, T. Sakai, T. Nakahira, M. Komori and K. Tsujimura. 1992. Measurement of Flame Temperature Distribution in D.I. Diesel Engine with High Pressure Fuel Injection, SAE Paper 920692.

[3] I. Celikten. 2003. An experimental investigation of the effect of the injection pressure on engine performance and exhaust emission in indirect injection diesel engines, Applied Thermal Engineering. 23(16): 2051-2060.

[4] C. H. Lee. 2008. An Empirical Correlation between Spray Dispersion and Spray Tip Penetration from an

[5] Edge Detection of Visualized Images under the Flow Condition of a Solid Body Rotating Swirl, Journal of Visualization. 11(1): 55-62.

[6] H. Hiroyasu. 1985. Diesel Engine Combustion and its Modeling, COMODIA. 85 53-75.

[7] H. Hiroyasu, T. Kadota and M. Arai. 1980. Fuel Spray Characterization in Diesel Engines Combustion Modelling in Reciprocant Engines, Mattavi and Amann, Plenum Press. 369-408.

[8] R. J. H. Klein-Douwel, P. J. M. Frijters, L.M.T. Somers, W. A. de Boer, R. S. G. Baert. 2007. Macroscopic diesel fuel spray shadowgraphy using high speed digital imaging in a high pressure cell, Fuel. 86(12-13): 1994-2007.

[9] Y. Zhang, T. Ito and K. Nishida. 2001. Characterization of Mixture Formation in Split-Injection Diesel Sprays via Laser Absorption-Scattering (LAS) Technique, SAE Paper 2001-01-3498.

[10] J. Gao, K. Nishida, S. Moon and Y. Matsumoto. 2009. Characteristics of Evaporating Diesel Spray: A Comparison of Laser Measurements and Empirical/Theoretical Predictions, SAE Paper 2009-01-0854.

[11] C. Du, M. Andersson, and S. Andersson. 2016. Effects of Nozzle Geometry on the Characteristics of an Evaporating Diesel Spray, SAE Paper 2016-01-2197.

[12] P. G. Felton, F. V. Bracco and M. E. A. Bardsley. 1993. On the Quantitative Application of Exciplex Fluorescence to Engine Sprays, SAE Paper 930870.

[13] F. Rabenstein, J. Egermann and A. B. Leipertz. 1998. Vapor-Phase Structure of Diesel-Type Fuel Sprays: An Experimental Analysis, SAE Paper 982543.

[14] M. A. M. Nawi, N. Uwa, Y. Ueda, Y. Nada and Y. Kidoguchi. 2015. Droplets Behavior and Evaporation of Diesel Spray Affected by Ambient Density after Pilot Injection, SAE Paper 2015-32-0724.

[15] F. Pischinger. 1962. Development Work on a Combustion System for Vehicle Diesel Engines, in FISITA Congress.

[16] G. Tippelmann. 1977. A New Method of Investigation of Swirl Ports, SAE Paper 770404.

[17] K. I. Kim and C. H. Lee. 2009. Development of a new swirl measurement method for an engine cylinder head by automating the swirl measuring process, Proc. IMechE, Part D: J. Automobile Engineering. 223(3): 375-387.

[18] D. S. Oh and C. H. Lee. 2019. Development of a new system for measuring the swirl ratio of an engine cylinder head under an unsteady flow condition, Journal of Mechanical Science and Technology. 33(2): 955-965.

[19] T. Uzkan, C. Borgnakke and T. Morel. 1983. Characterization of Flow Produced by a High Swirl Inlet Port, SAE Paper 830266.